



Reflective Focusing Based on Few-Layer Gradient Metasurface Element Array

Mengyao Yan, Zhichao Sun, Bairui Wu, Pan Cheng and Bijun Xu*

School of Science, Zhejiang University of Science and Technology, Hangzhou, China

This study proposes a three-layer focusing gradient metasurface for wavefront processing. The structure works in the frequency range of 15–25 GHz and has a central frequency of 19.6 GHz. The metasurface unit is organized in a square and has high-impedance elements that reflect the full range of phase shifts. When the microwave beam is incident on this metasurface, the high-impedance elements modulate the beam according to the gradient arrangement, to realize the focusing effect of the lens, and the efficiency reaches 82%. The simulation results are consistent with the theoretical results.

Keywords: metasurface, reflective, focus, wavefront, simulation

OPEN ACCESS

Edited by:

Yuancheng Fan,
Northwestern Polytechnical
University, China

Reviewed by:

Xiangping Li,
Jinan University, China
Zhengren Zhang,
Chongqing Jiaotong University, China
Rui-Pin Chen,
Zhejiang Sci-Tech University, China

*Correspondence:

Bijun Xu
xubijun@zust.edu.cn

Specialty section:

This article was submitted to
Optics and Photonics,
a section of the journal
Frontiers in Physics

Received: 28 December 2019

Accepted: 20 February 2020

Published: 20 March 2020

Citation:

Yan M, Sun Z, Wu B, Cheng P and
Xu B (2020) Reflective Focusing
Based on Few-Layer Gradient
Metasurface Element Array.
Front. Phys. 8:46.
doi: 10.3389/fphy.2020.00046

INTRODUCTION

The acquisition of new materials with new optical properties has become an important research field [1]. People acquire new materials by chemical synthesis [2], and they manipulate the optical properties by artificially designing dielectric constants and magnetic permeability [3, 4]. The degree of freedom and maneuverability of the artificial optical structure is higher than that of chemical synthesis methods [5]. From 2000 to 2010, the use of metamaterials to design new optical devices and achieve unique optical functions has received significant attention. Examples of these include negative refraction, metalenses, optical stealth cloaks, and artificial chirality [6, 7].

Fermat's principle [8] points out that the wavefront of a light beam can be modified by controlling the phase of the light wave [9, 10]. A metasurface exhibits peculiar optical properties in controlling electromagnetic waves [11, 12]; it is also widely used in the terahertz band [13]. Traditional metal-based metasurfaces can effectively reduce losses during electromagnetic wave propagation [14, 15], but the interaction intensity decreases as the distance between the metasurface and the electromagnetic beam increases [16, 17]. The metal—medium—metal structure [18] provides an effective way to achieve efficient control of light wave amplitude, phase, and polarization [19]. In this study, we propose and validate a new type of focusing lens based on a three-layer square gradient metasurface reflector array, which can approximate and the reflection phase in the range of 2π by controlling the metasurface unit.

MODEL DESIGN

As shown in **Figure 1A**, an element of the metasurface array has three layers, and the metal layers use a perfect electrical conductor (PEC). Metals behave like PEC in the microwave band and a reflectarray built using elements of variable dimensions can reflect the incident waves with high efficiency. As shown in **Figure 1B**, the top metallic patch layer is a square that is hollowed from the inside to the outside. **Figure 1C** shows the element parameters. The thickness of each metal layer and the dielectric are $t = 0.035$ mm and $h = 1.60$ mm, respectively, and the dielectric constant

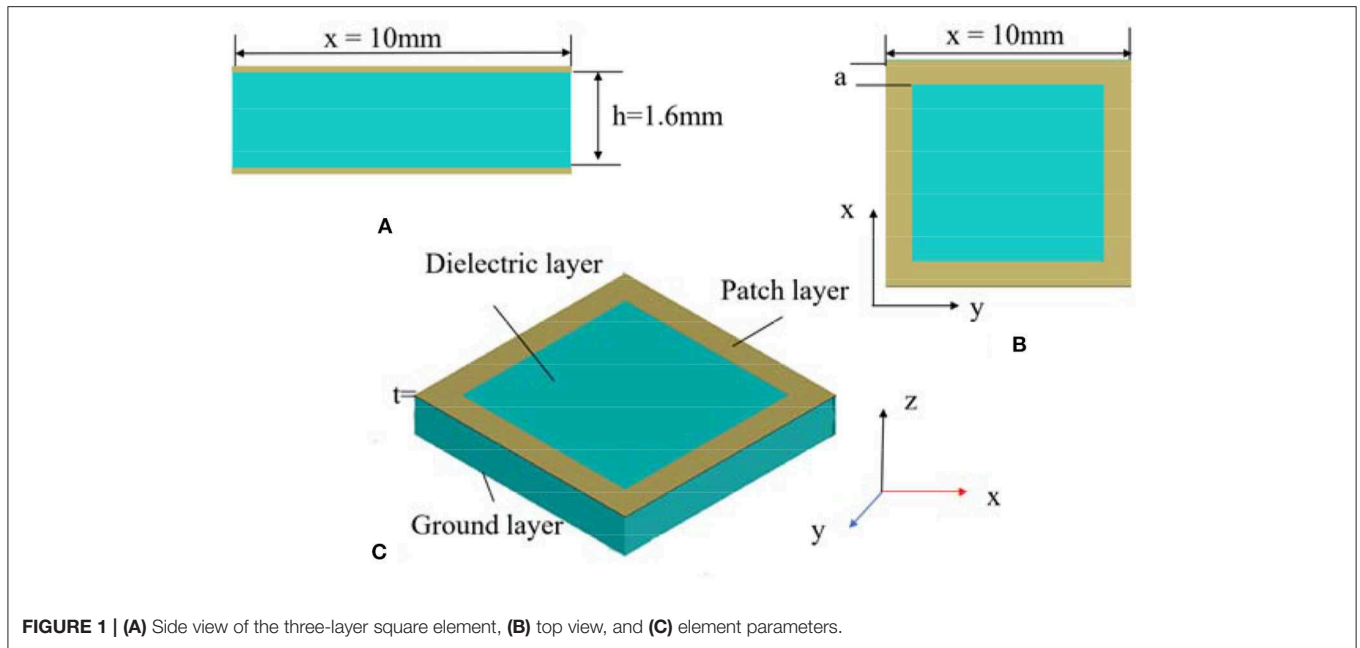


FIGURE 1 | (A) Side view of the three-layer square element, (B) top view, and (C) element parameters.

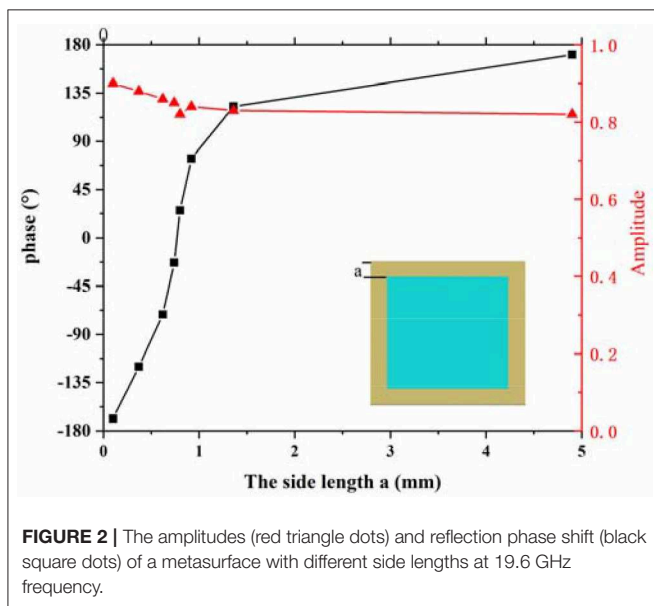


FIGURE 2 | The amplitudes (red triangle dots) and reflection phase shift (black square dots) of a metasurface with different side lengths at 19.6 GHz frequency.

$$f(x, y) = \frac{2\pi}{\lambda_0} (\sqrt{x^2 + y^2 + f^2} - f) + f_0 \quad (1)$$

Where f is the focal length, and λ_0 is the free-space wavelength [23, 24].

A continuous curve of phase shift in the range of -168.5° to 170.8° , as shown in **Figure 2**, can be achieved by changing the width of the metallic patch layer. The maximum range of the phase shift can reach 339° , which is close to a full cycle and sufficient for the intended operation of a reflectarray while maintaining the amplitude of the reflected wave above 0.82. The focal length is 150 mm. As shown in **Figure 3**, the three-layer metasurface array consisted of 13×13 square elements. The desired phase shift is obtained by just changing the inner radius parameter of the metallic patch. The radii of the patches in the eight parts are 0.1, 0.37, 0.62, 0.74, 0.80, 0.92, 1.36, and 4.9 mm, respectively. The element can be used for a metasurface lens with good performance. The reflection phases of the eight concentric parts fulfill Equation (1).

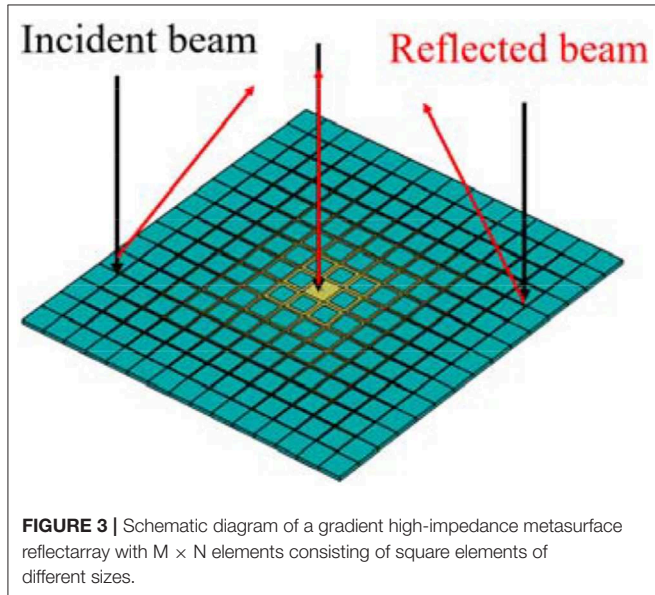
RESULTS AND DISCUSSION

The CST Microwave Studio software was used to solve the reflection spectra of the metasurface structure. The plane wave propagated in the negative z direction and linearly polarized along the direction of incidence of the beam. The simulation results are shown in **Figure 4**. **Figure 4A** shows the reflected electric-field intensity distribution in the x - y plane, where the focal length f is ~ 146 mm. **Figure 4B** shows the reflection intensity distribution in the x - y plane at $z = 146$ mm, $z = 150$ mm, and $z = 170$ mm, respectively. One can see that the energy is the strongest, the light spot is the smallest, and the focusing effect is the best at $z = 146$ mm. **Figure 4C** shows

is 2.60. The lattice constant is $x = 10$ mm. The width of the metallic patch is the only adjustable parameter, and it has a significant influence on the reflection phase. By changing the value of the parameter, it is possible to control the incident beam and make it converge at one point.

Compared with other focusing structures [20, 21], the thickness of the proposed design only is 1.67 mm, which is much smaller than the operational wavelength. It is easy to manufacture. The phase (ϕ) distribution of the focusing gradient metasurfaces usually follows Equation (1) [22].

the 3D radiation pattern at 19.6 GHz, and **Figure 4D** shows the electric-field energy density distribution in the x - z plane. Focus conversion efficiency was $\sim 82\%$. The calculation method is the ratio of focus energy of the focal spot to the total

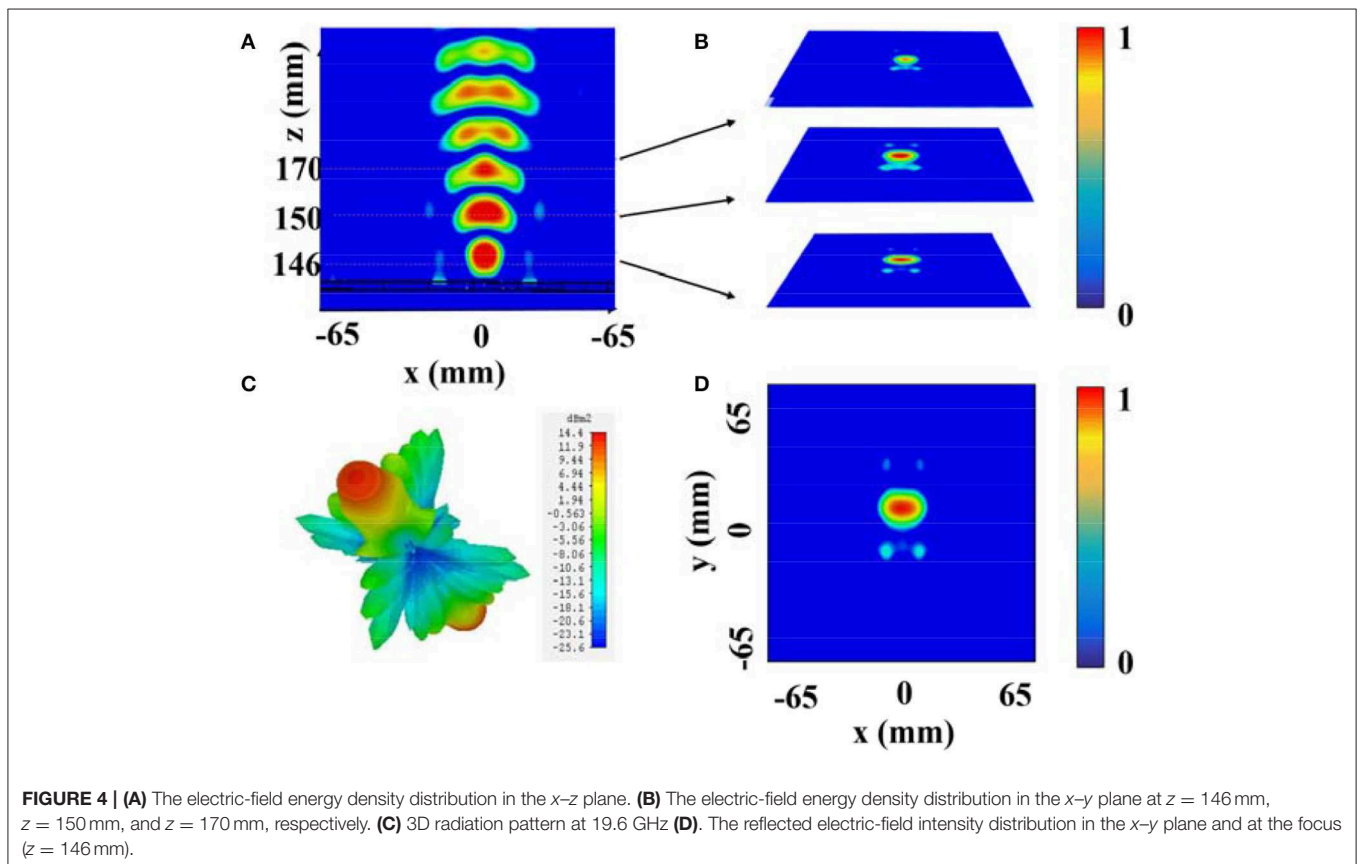


energy of the incident wave. Owing to the good focusing performance, the proposed array can achieve a pencil-shaped radiation pattern.

It is reasonable to infer that the high-efficiency focusing has a broadband characteristic. As shown in **Figure 5**, the results of near-field distribution at 18, 19, and 20 GHz show a high focusing efficiency over a wide frequency range. **Figures 5B,E,H** and **Figures 5C,F,I** show that the focal length increases and the far-field radiation decreases with the decrease of working frequency. Specifically, the focal length is 150 mm at 18 GHz, the far-field value is 13.7 dB, the focal length is 110 mm at 19 GHz, the far-field value is 14.5 dB, the focal length is 90 mm at 20 GHz, and the far-field value is 14.7 dB. The simulation results verify the hypothesis and show a wide broadband of operation, and the demonstrated high efficiency and broadband wavefront steering can be applied in imaging and high-directional antennas.

CONCLUSION

A three-layer square reflective array was simulated based on a focused gradient metasurface. In the microwave frequency band, the reflection phase of a single element to electromagnetic waves varies only with the width of the metallic patch layer. The phase discontinuity on the metasurface depends only on the precise control of the three-layer square elements



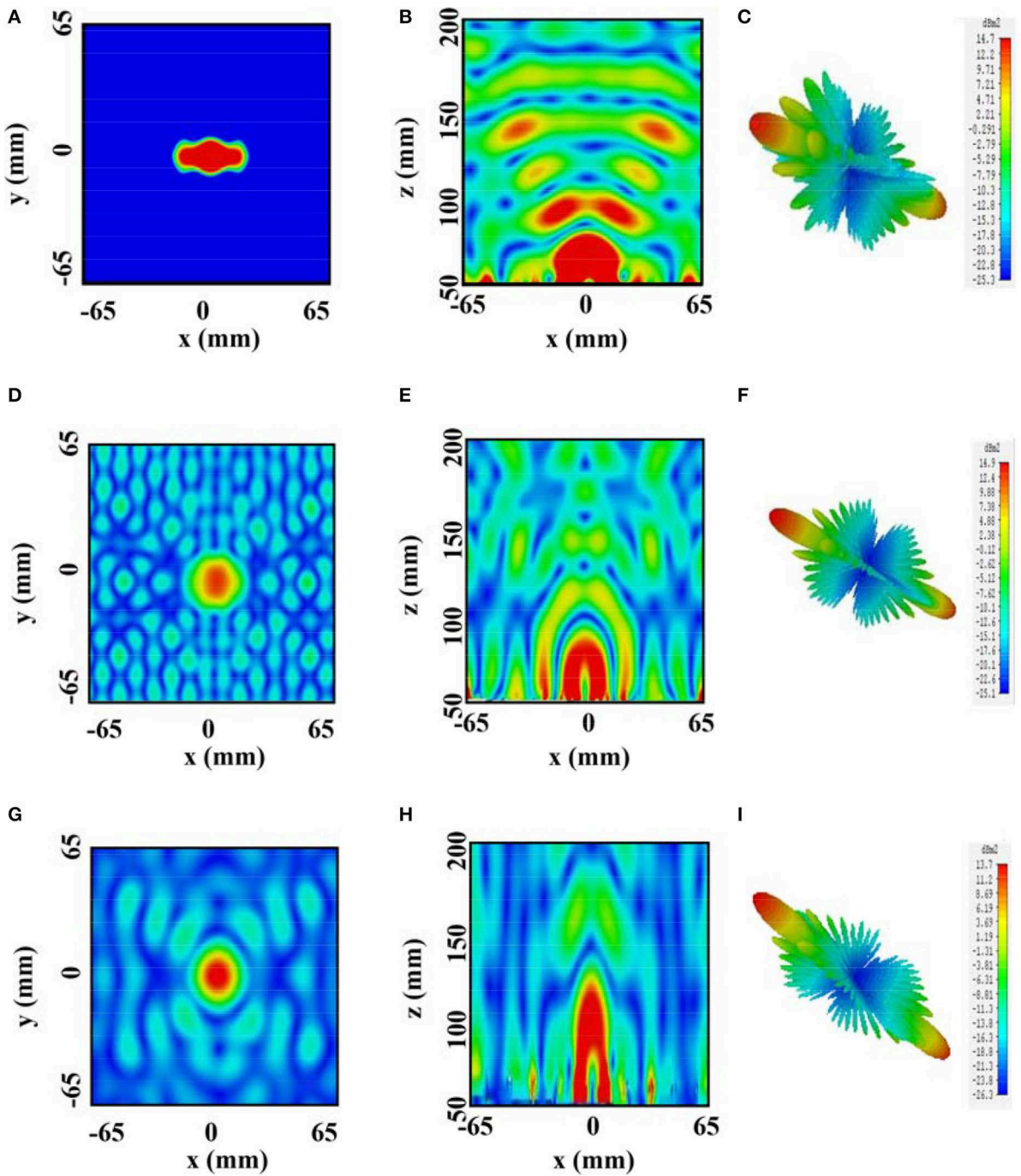


FIGURE 5 | The field intensity, distribution in the y - z plane, x - y plane, and 3D radiation pattern at 20 GHz (A-C), 19 GHz (D-F), and 18 GHz (G-I), respectively.

in a subwavelength dimension, in which the size of the square metasurface has a linear relationship with the phase discontinuity. The proposed gradient metasurface can be used for the realization of approximately full range reflection phase shift modulation, and the simulation results show that the three-layer gradient metasurface reflection array has a good

focusing efficiency of 82%. In addition, because of the simple structure of the components, the three layers can be made of common materials, which makes the device convenient to design and manufacture. It provides a new method for the design of passive-reflection focusing arrays, which improves the guiding efficiency of electromagnetic beams.

AUTHOR CONTRIBUTIONS

BX developed the concept and supervised the whole project. MY carried out the simulations and analyzed the simulation data. BX and ZS contributed to writing and finalizing the paper. BW and PC contributed to paper revision and language editing.

ACKNOWLEDGMENTS

The simulation software and writing assistance were provided by BX. The laboratory support was provided by School of Sciences, Zhejiang University of Science and Technology.

REFERENCES

- Pfeiffer C, Grbic A. Controlling vector Bessel beams with metasurfaces. *Phys Rev A*. (2014) 2:044012. doi: 10.1103/PhysRevApplied.2.044012
- Lin D, Fan P, Hasman E, Brongersma ML. Dielectric gradient metasurface optical elements. *Science*. (2014) 345:298–302. doi: 10.1126/science.1253213
- Ni X, Kildishev AV, Shalaev VM. Metasurface holograms for visible light. *Nat Commun*. (2013) 4:2807. doi: 10.1038/ncomms3807
- Tamilchelvan R, Senthilkumar VJ. Design and optimization of wideband microwave amplifier using nonlinear technique. *Wirel Pers Commun*. (2018) 99:1589–604. doi: 10.1007/s11277-018-5293-5
- Asadchy VS, Díaz-Rubio A, Tretyakov SA. Bianisotropic metasurfaces: physics and applications. *Nanophotonics*. (2018) 7:1069–94. doi: 10.1515/nanoph-2017-0132
- Zheludev NI. The road ahead for metamaterials. *Science*. (2010) 328:582–3. doi: 10.1126/science.1186756
- Liu L, Ding Y, Yvind K, Hvam JM. Silicon-on-insulator polarization splitting and rotating device for polarization diversity circuits. *Opt Express*. (2011) 19:12646–51. doi: 10.1364/OE.19.012646
- Ding F, Yang Y, Deshpande RA, Bozhevolnyi SI. A review of gap-surface plasmon metasurfaces: fundamentals and applications. *Nanophotonics*. (2018) 7:1129–56. doi: 10.1515/nanoph-2017-0125
- Chou HC, Tung NL, Kehn MNM. The double-focus generalized luneburg lens design and synthesis using metasurfaces. *IEEE Trans Antennas Propag*. (2018) 66:4936–41. doi: 10.1109/TAP.2018.2845550
- Yun H, Chrostowski L, Jaeger NAF. Ultra-broadband 2×2 adiabatic 3 dB coupler using subwavelength-grating-assisted silicon-on-insulator strip waveguides. *Opt Lett*. (2018) 43:1935–8. doi: 10.1364/OL.43.001935
- Cai W, Shalaev VM. *Optical Metamaterials*. New York, NY: Springer (2010). doi: 10.1007/978-1-4419-1151-3
- Fu Y, Shen C, Cao Y, Gao L, Chen H, Chan CT. Reversal of transmission and reflection based on acoustic metagratings with integer parity design. *Nat Commun*. (2019) 10:2326. doi: 10.1038/s41467-019-10377-9
- Barwicz T, Watts MR, Popović MA, Rakich PT, Succi L, Kärtner FX, et al. Polarization-transparent microphotonic devices in the strong confinement limit. *Nature photonics*. (2007) 1:57–60. doi: 10.1038/nphoton.2006.41
- Wang Y, Ma M, Yun H, Lu Z, Wang X, Jaeger NA, et al. Ultra-compact sub-wavelength grating polarization splitter-rotator for silicon-on-insulator platform. *IEEE Photonics J*. (2016) 8:1–9. doi: 10.1109/JPHOT.2016.2630849
- Ding Y, Ou H, Peucheret C. Wideband polarization splitter and rotator with large fabrication tolerance and simple fabrication process. *Opt Lett*. (2013) 38:1227–9. doi: 10.1364/OL.38.001227
- Zhang Z, Yang Q, Gong M, Chen M, Long Z. Metasurface lens with angular modulation for extended depth of focus imaging. *Opt Lett*. (2020) 45:611–4. doi: 10.1364/OL.382812
- Zhang Z, Yang Q, Gong M, Long Z. Toroidal dipolar bound state in the continuum and antiferromagnetic in asymmetric metasurface. *J Phys D Appl Phys*. (2019) 53:075106. doi: 10.1088/1361-6463/ab5983
- Shi Z, Khorasaninejad M, Huang YW, Roques Cames C, Zhu AY, Chen WT, et al. Single-layer metasurface with controllable multiwavelength functions. *Nano Lett*. (2018) 18:2420–7. doi: 10.1021/acs.nanolett.7b05458
- Xu B, Wei Z, Wu C, Fan Y, Wang Z, Li H. Near-diffraction-limited focusing with gradient high-impedance metasurface. *Opt Mater Express*. (2017) 7:1141–6. doi: 10.1364/OME.7.001141
- Dong X, Sun H, Gu CQ, Li Z, Chen X, Xu B. Generation of ultra-wideband multi-mode vortex waves based on monolayer reflective metasurface. *Prog Electromagn Res*. (2019) 80:111–20. doi: 10.2528/PIERM19010504
- Wang H, Li Y, Han Y, Fan Y, Sui S, Chen H, et al. Vortex beam generated by circular-polarized metasurface reflector antenna. *J Phys D Appl Phys*. (2019) 52:255306. doi: 10.1088/1361-6463/ab1742
- Chrostowski L, Hochberg M. *Silicon Photonics Design: From Devices to Systems*. Oxford: Cambridge University Press (2015). doi: 10.1017/CBO9781316084168
- Fan Q, Huo P, Wang D, Liang Y, Yan F, Xu T. Visible light focusing flat lenses based on hybrid dielectric-metal metasurface reflector-arrays. *Sci Rep*. (2017) 7:45044. doi: 10.1038/srep45044
- Sun Z, Mengyao Y, Mupona TE, Bijun X. Control electromagnetic waves based on multi-layered transparent metasurface. *Front Phys*. (2019) 7:181. doi: 10.3389/fphy.2019.00181

Conflict of Interest: The authors declare that the research was conducted in the absence of any commercial or financial relationships that could be construed as a potential conflict of interest.

Copyright © 2020 Yan, Sun, Wu, Cheng and Xu. This is an open-access article distributed under the terms of the Creative Commons Attribution License (CC BY). The use, distribution or reproduction in other forums is permitted, provided the original author(s) and the copyright owner(s) are credited and that the original publication in this journal is cited, in accordance with accepted academic practice. No use, distribution or reproduction is permitted which does not comply with these terms.